

Detection of Geological Structures in the Gol Gohar Mining Iron Ore Area Using Airborne Magnetic Data

Abdullah Ezam Ahmady ¹, Abdolhamid Ansari ¹, Seyyed Hossein Mojtahedzadeh ¹

¹ Dept. of Mining and Metallurgy Engineering, Yazd University, Yazd, Iran

* Corresponding Author: h.ansari@yazd.ac.ir

Receive Date: 16 November 2024

Accept Date: 22 January 2025

DOI: **10.22034/ANM.2025.22369.1647**

This is an "accepted before publication" version of the paper that has been deemed acceptable for publication in the Journal of Analytical and Numerical Methods in Mining Engineering after the judging process. This version will be published online after the announcement of acceptance and before the editing process. The article, after the final preparation and publication process, will be removed from the accepted version before

Abstract

This study focuses on the analysis of airborne magnetic data to identify surface and subsurface structures at various depths within the Gol Gohar mining area. The Gol Gohar region is recognized as one of the active mining areas in Iran, comprising six major anomalies along with several minor anomalies that contribute to significant complexities in its geological structures. Despite numerous studies conducted in this area, its deeper structures have not been thoroughly examined.

The data utilized in this study consists of airborne magnetic data, with a line spacing of 500 meters and an average flight altitude of 120 meters. The methodology of this research begins with the application of the Reduced to the Pole (RTP) filter, utilizing Fast Fourier Transform (FFT) techniques to distinguish local residual structures from broader regional features. This multiscale approach facilitates a deeper understanding of the geological complexities within the study area and clearly reveals its subsurface structures. Subsequently, advanced geophysical methods such as Total Horizontal Derivative (TDHR) and Tilt Angle Derivative (TDR) are employed to delineate the boundaries of anomalies. The objective of employing these methods is to delineate the structural boundaries of magnetic anomalies. Additionally, an advanced method for estimating the depth of magnetic anomalies, known as Euler Deconvolution, has been employed.

Interpretations derived from the airborne magnetic data indicate that the geological structures generally trend NW-SE and are disrupted and offset by a series of faults with an approximately N-S orientation. Furthermore, the results suggest that ferromagnetic bodies are situated at considerable depths, extending from the NW towards the SE. This study is particularly important for identifying the magnetic anomaly structures in the Gol Gohar mining area, as it not only reveals the concealed anomalies of this mineral-rich region but also clarifies the arrangement of these anomalies effectively.

Aeromagnetic data, Edge detectors, Structural features, Euler Method, Gol Gohar Mining complex

1. Introduction

The Gol Gohar mining area, endowed with rich iron ore deposits, stands as one of the most prominent active mining and industrial hubs in the Middle East. These mineral reserves are located in Kerman Province, approximately 50 kilometers southwest of Sirjan County. The GolGohr iron ore deposit comprises six distinct anomalies, collectively estimated to contain around 1,200 million tons of ore, spanning an approximate length of 10 kilometers and a width of about 4 kilometers.

Despite extensive mining activities conducted over the years, the deep geological status of the area regarding ore formation and the structural relationships of the identified masses remains inadequately understood, leading to significant ambiguities. The structural relationship among these mineral bodies poses a geological uncertainty that, if resolved, could enhance the discovery of new deposits, inform extraction planning, and aid in the determination of waste rock storage locations.

Extensive geological and geophysical studies have been conducted, alongside the identification of numerous near-surface anomalies. It is anticipated that if there is a possibility of new bodies existing between the known masses, these bodies are likely to be located at greater depths than the conventional depths of the existing bodies in the region. Consequently, the exploration of deep ore deposits becomes a pertinent issue. Deep ore exploration presents numerous complexities and challenges compared to near-surface deposits and necessitates the application of geophysical methods that allow for deeper investigations than conventional techniques.

Among the most commonly used methods of enhancing magnetic anomalies are reduction to pole (RTP), analytic signal (AS), and total horizontal gradient (THDR) [1]. Applying derivatives of magnetic data in 2004 by Bruno Verduzco could study the structures of anomalies [2]. Normalized derivatives offer geophysicists an innovative set of images that, when applied appropriately, can enhance the identification and mapping of geological structures derived from magnetic data [3]. Sultan, and et al. used magnetic data for subsurface structures by applying Euler deconvolution and horizontal gradient [4, 5]. Oruç and Selim, employed tilt angle derivatives and Euler deconvolution methods to determine the characteristics of magnetic lineaments in the central Black Sea region [6]. Ferreira and et al, utilized horizontal gradient derivatives and tilt angle analysis of magnetic data to delineate the edges of magnetic anomalies [7]. Modern exploration methods are able to measure small changes in the earth's geophysical features using sensitive platforms and instruments that have high accuracy with innovative data processing techniques[8]. In areas with limited exposure, aeromagnetic surveys have become a crucial component of exploration programs[9]. By applying vertical derivatives (VDR), analytic signal (AS) amplitude, and horizontal derivative of the tilt derivative (TDR_THDR) subsurface structures were studied by[10]. Nasuti1 and Nauti2, developed a new phase – based filter to enhance the edges of geologic sources which utilizes the vertical derivative of analytical signal in different orders to the tilt derivative equation [11]. Ibraheem, and et al. analyzed magnetic data to detect the structures by applying RTP, Euler deconvolution, VDR and TDR_THDR filters to magnetic data [12]. One of the goals of geophysical data processing is to separate distinct signals from different geological bodies, such as large bodies from small bodies or deep bodies from shallow bodies[13-15]. Derivative-based techniques are widely regarded as one of the most effective approaches for identifying the horizontal positions of potential subsurface structures in geophysical research domains [16]. The presence of abnormal magnetic field is a necessary condition for detecting magnetic anomalies[17].

Previous studies in various countries have demonstrated that the interpretation and analysis of magnetic data can be used to identify deep geological structures. However, in the study area, which features a highly complex and intricate tectonic structure, magnetic data have not yet been explicitly and accurately utilized to investigate deep structures. This issue arises from the numerous ambiguities surrounding the deep structures of the anomalies; for instance, it remains unclear whether these structures converge at a fixed anomaly depth or if the molten materials responsible for the formation of iron ore deposits have ascended separately through faults without any deep-seated connections.

Therefore, this research aims to explore the deep geological relationships of the Gol Gohar structures using magnetic data and their analysis and interpretation. The methods deemed effective for achieving the objectives of this study include gradient derivative methods, tilt angle analysis, and Euler deconvolution techniques. These methods are capable of delineating the boundaries of anomalies beneath the Earth's surface, and the results obtained can significantly contribute to identifying the subsurface geological structures associated with the Gol Gohar anomalies.

The case study of this research is the mining area of Gol Gohar (Figure 1). This mining area is located in the southern part of Sanandaj-Sirjan zone. This mining area is a metamorphic zone that is a collection types of schist, amphibolite, gneiss, carbonate rocks and marble outcrops that covered by young alluvial and destructive deposits[18]. Many exploratory and mining studies have been carried out in this mining area, but until now, the deep structures of these anomalies have not been considered together as a mass, whether these deep structures have a deep relationship from the point of view of geology and tectonics or not. Therefore, this research has been done with the aim of determining the depth of Gol Gohar anomalies based on the airborne magnetic field data.

2. Aeromagnetic data

2.1. Source Data

Airborne magnetic data used in this research was collected by the Aero Service of Canada in 1976 with a line distance of 500 meters and a height of 120 meters. The dimensions of the studied area are 12.5 x 14 km, which covers about 156 square kilometers. The average value of inclination and declination in this area is 43.2832° and 0.409° respectively. Using the International Geomagnetic Reference Field (IGRF), the geomagnetic gradient was removed, and the Residual Magnetic Field was obtained.

2.2. Geological Setting

The 1:25000 geological map of Gol Gohar with an area of 156 Km² is located in 53 Km southwest of Sirjan, southwest of Kerman, Iran (Fig. 1). It is structurally situated in Sanandaj-Sirjan metamorphic zone. It is characterized by a variety of middle Jurassic metamorphic rocks including schist, amphibolite's, gneiss, crystallized limestone's and marbles. In addition to these rocks, the area is approximately predominated by young detrital and alluvial deposits. The magnetite-bearing ore is classified into two primary morphological types: massive and banded, with the banded variety predominantly found within magnesian marble host rocks. Both subtypes exhibit distinct mineral assemblages that include calcite, dolomite, forsterite, tremolite-actinolite, talc, serpentine, and chlorite. The principal ore minerals identified in both types are magnetite and hematite, accompanied by trace quantities of pyrite, pyrrhotite, and chalcopyrite[19].

Preliminary mechanism of older faults in the area is mostly reverse strike-slip. Joint studies have shown predominant NE-SW fracturing of the same component as faults (reverse strike-slip) in the eastern part of the area. Most of the Pliocene-Quaternary faults display NW-SE and W-E trending. Structural analyses demonstrate that at least in Pliocene-Quaternary, the studied area has been substantially subjected to normal lateral strike-slip and strikeslip movements and has not been noticeably affected by compressional tectonism. According to these studies, it appears that the NE-SW shortening regimen is replaced with extensional regimen, bringing about subsequent normal faulting and metamorphic rocks outcropped in GoleGohar area. According to the geochemical studies conducted, schists and amphibolite's do not contribute to the formation of Gol Gohar iron deposit and are only intrusive rocks. Based on studies and isotopic measurements, the age of Gol Gohar iron deposit is estimated to be 349 to 355 million years (Lower Carboniferous) and the origin of Gol Gohar iron deposit is believed to be magmatic fluids [20, 21].

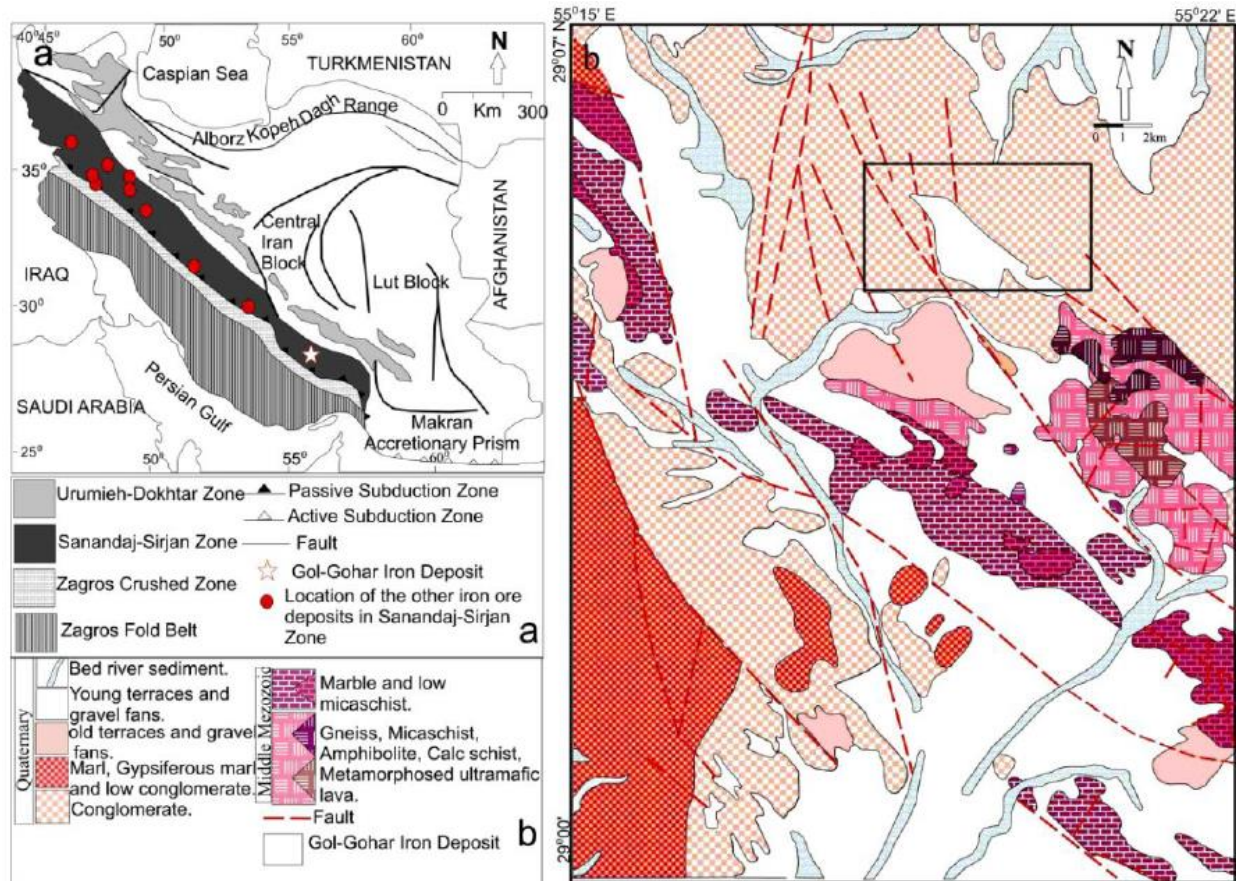


Fig.1. Geological Map of Gol Gohar (1:25000)[19].

3. Methodology and Approaches

Magnetic imagery serves as a tool for identifying regions of significant magnetic contrast and for visualizing geological features such as faults and dykes, which are represented as lineaments. The amplitude of magnetic anomalies is influenced by both the strength of the magnetic field and the depth of the anomalous sources; consequently, lower amplitude anomalies may be obscured in favor of higher amplitude signals[12]. While the filtered data may exhibit quantitative distortions, the efficacy of separation filtering in qualitative analysis continues to be robust, serving as a valuable tool for anomaly detection and pattern differentiation[22, 23].

To address this issue, edge-detection filters are employed to delineate linear features while preserving long-wavelength information. Among these, the Total Derivative Ratio (TDR) filter is particularly noteworthy as an effective edge-detection tool.

The tilt angle derivative and total horizontal gradient methods perform well in identifying the location of geological structures; however, the Euler deconvolution method provides higher accuracy in estimating the depth of these structures. All three methods require high-quality data, but the tilt angle derivative and horizontal gradient methods are more sensitive to noise, whereas the Euler deconvolution method is less affected by it. Therefore, the Euler deconvolution method is better suited for precise modeling and estimation of the depth and position of subsurface structures, while the tilt angle derivative and horizontal gradient methods are more effective for detecting surface boundaries[7, 24].

3.1. Reduced to magnetic pole

Magnetic anomalies are typically bipolar in nature, and neglecting this characteristic can lead to significant errors in data analysis, particularly in determining the locations of anomalous bodies. The aim of reducing to the pole is

to determine the anomaly that would be detected if the magnetic field were oriented vertically, typically under the assumption of ideal induction for ease of calculation[25]. One effective method for processing magnetic data is the pole-reversal transformation. During this stage, the effects of bipolar anomalies are eliminated, allowing the anomalies to manifest as monopolar. The resulting pole-reversed maps can be utilized to accurately identify the locations of ferromagnetic bodies[26].

3.2. Derivative Filters

Derivatives or gradients of magnetic fields are more sensitive to variations in magnetic field intensity. These filters are employed to enhance boundary details. They play a crucial role in isolating regional anomalies and residuals, as well as in estimating the boundaries of magnetic bodies.

3.2.1. Analytic Signal Derivative

The analytic signal filter is applied to estimate the boundaries of bodies, with the maximum value of the analytic signal corresponding to the edges of these bodies. The advantage of this method lies in its dependence on both the magnetization vector of the body and the Earth's magnetic vector [27, 28].

3.2.2. Total Horizontal Derivative (TDHR)

The objective of directional derivatives of potential field data is to derive them in the x and y directions. Directional derivatives are utilized to accentuate linear structures present in the maps. Anomalies identified through this method will be highlighted perpendicular to the direction of the derivative computation.

3.2.3. Tilt angle Derivative (TDR)

Miller and Singh (1994) demonstrated that the Total Derivative Angle (TDR) transitions through zero at or near the boundary of a vertically-sided source, exhibiting negative values in areas outside the source region. This property makes the TDR particularly effective for tracing anomalies along their strike. Additionally, Verduzco et al. (2004) highlighted that the TDR functions as an automatic gain control (AGC) filter, which helps to normalize the response from both weak and strong anomalies, enhancing the clarity of the data interpretation. The tilt derivative, also referred to as the tilt angle, was initially introduced by [29] as a method for identifying magnetic sources within magnetic profile data. The horizontal gradient magnitude (HGM) is mathematically defined as the square root of the sum of the squares of the horizontal derivatives of the potential field f :

$$HGM = \sqrt{\left(\frac{df}{dx}\right)^2 + \left(\frac{df}{dy}\right)^2}. \quad (1)$$

Where df/dx and df/dy are the first derivatives of the field f in the x and y directions. Verduzco et al, 2004 expanded the concept to facilitate its application to grid data by introducing a generalized tilt derivative defined as:

$$TDR = \tan^{-1} \left(\frac{\frac{df}{dz}}{HGM} \right), \quad (2)$$

Where df/dz is the first vertical derivative of the field f .

3.3. Euler deconvolution

The Euler deconvolution method was first introduced by [30] by writing the Euler homogeneity equation and deriving the structural index as a measurement of the rate of change with the distance of a field. [31] studied and implemented this method for synthetic and real magnetic data along profiles. Euler's semi-automatic deconvolution method uses the magnetic field and its three orthogonal gradients (one vertical and two horizontal) to estimate the depth of the magnetic anomaly source. The sampling of this magnetic field is interpolated from the original data distribution on a

rectangular grid[32]. Euler deconvolution method depth estimation can be implemented by Oasis Montaj program, this program allows the selection of several parameters including the structural index, the size of the depth tolerance window and the distance, and also allows the interpreter to change the value of these parameters[33].

According to the theory of [34], Euler's three-dimensional equation has the following form:

$$(x - x_0) \frac{\partial T}{\partial x} + (y - y_0) \frac{\partial T}{\partial y} + (z - z_0) \frac{\partial T}{\partial z} = N(B - T) \quad 3$$

In this equation, $\partial T/\partial x$, $\partial T/\partial y$, and $\partial T/\partial z$ are the derivatives of the field in the x, y, and z directions, B is the plane level of the field, and N is the Structural index, which is selected from the range based on the previous values.

The location of the source (X_0, Y_0, Z_0) and B can be calculated based on the linear equations according to equation 3. In equation 3, N is the structural index that calculates the rate of reduction of the amplitude response with the distance from the source. The structural index has an effect on the measured slope and is related to the anomalous geometry. The structural index for the magnetic spherical source is 3. The structural index is between 0 and 3 for different types of resources, which cannot be zero. For high depths, N is considered high and for very shallow depths, N is considered too low. One of the main reasons for the error in Euler deconvolution is that the gradient in the transverse line is limited due to the spatial asymmetry in the sampling[9].

Since the quality of depth estimation by Euler's method is related to the appropriate selection of the structural index, which is a function of the geometry of the causative objects, and Euler's deconvolution method is only used for homogeneous functions. On the other hand, many complex geological structures can be approximated as functions such as thin dikes, contacts and horizontal cylinders. Therefore, the structural index for contact models will be 1, for a sheet model it will be 2, and for a horizontal cylinder it will be 3, which is one more than the structural indices for the anomalies of the corresponding field[32].

4. Result and Discussion

The interpretation of aeromagnetic data is considered a valuable method for identifying geological structures. This approach serves as a fundamental tool for geologists and geophysicists in the identification of subsurface geological formations, providing a reliable framework for mineral exploration [35]. Derivative-based methods are recognized as efficient and rapid tools for analyzing magnetic networks and providing precise information regarding structural settings, tectonic processes, and subsurface depths [12]. However, the complexity of the structural conditions in the Gol Gohar region necessitates the implementation of an integrated approach utilizing multiple edge-detection techniques.

4.1. Residual magnetic Intensity (RES) and Reduced to Magnetic pole (RTP) map results

This map is generally divided into two main sections (Fig2.a). The first section, extending from the northwest to the southeast in the northern part of the map, pertains to the magnetic anomalies associated with positive and negative poles. These anomalies indicate significant variations in the magnetic properties of the region and clearly reveal the diversity and complexities of its geological features. The second section of the map, encompassing the central and southern areas, likely refers to the bedrock and lithological variations. In this section, red is the dominant color, which does not specifically indicate magnetic anomalies with positive and negative poles. In contrast to the northern section, which is marked by both red and blue colors, this area displays only red. An increasing trend of lithological variations is reflected from the southern region towards the northern part of the map.

The RTP map, presented in (Fig.2b), has enhanced the clarity of magnetic anomalies by eliminating the magnetic field inclination across the region, thereby providing a more precise interpretation of lithological variations. This map has removed the positive monopolar anomalies located at the northernmost part of the figure (2.b), facilitating the interpretation of magnetic anomalies. Furthermore, the RTP map not only offers a clearer representation of the positive and negative poles of the magnetic anomalies but also distinguishes these anomalies from other parameters present in the map.

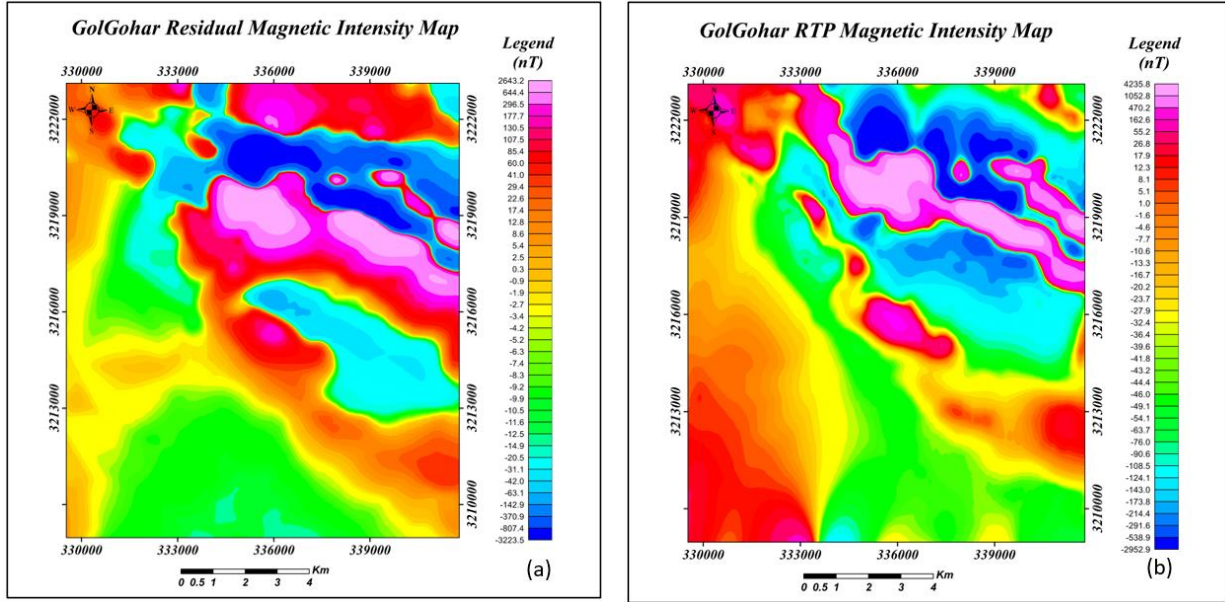
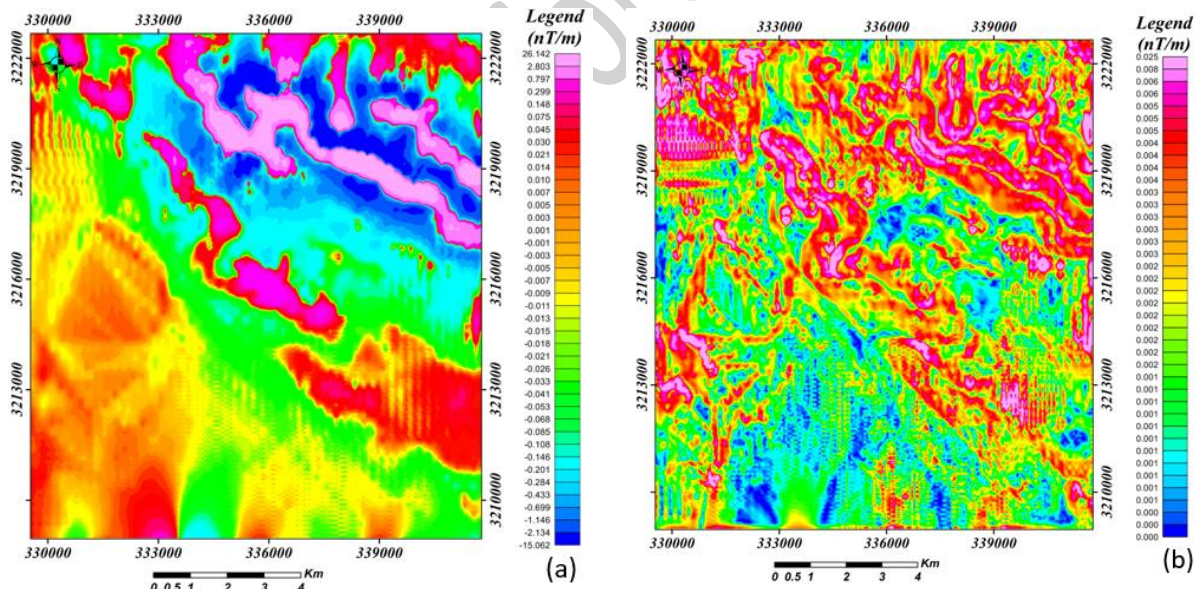


Figure 2. Gol Gohar RTP and RES grid map; Fig. 2. a. RES Magnetic Intensity Map; Figure 2. b. RTP Magnetic Map

4.2. Derivative-based methods results

In this study, various filters have been employed to identify the edges of magnetic sources associated with shallow and deep structures (including contacts, faults, and dikes) using RTP magnetic data. These filters include vertical derivative (VDR), Total horizontal derivative (TDHR), analytical signal (AS), Tilt Derivative angle (TDR) (illustrated in Figures 3a–d).



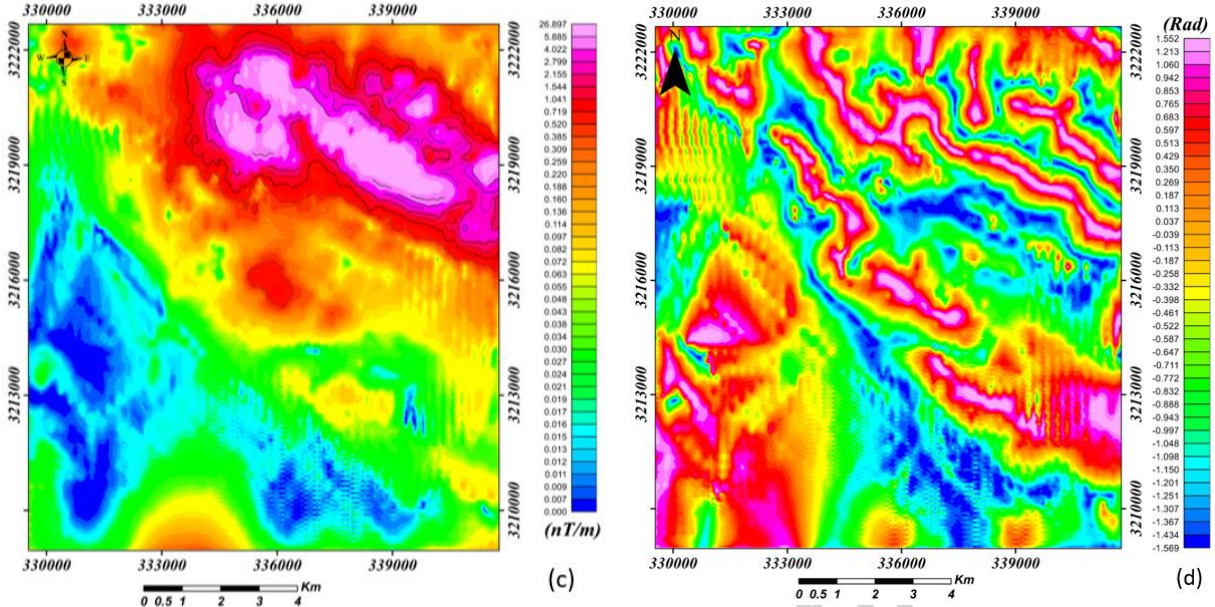


Figure 3. Derivative based map; Fig. 3a. vertical derivative (VDR); Fig.3b. total horizontal derivative THDR; Fig.3c. analytical signal (AS); Fig.3d. tilt angle (TDR)

Based on the observations presented in Figure 3, structural boundaries such as contacts/ faults are implicitly identifiable in these images. However, to more clearly delineate these boundaries and regional structures, TDR and THDR have been utilized, manifesting as structural lineaments. These methods enable us to analyze and identify geological features and existing boundaries in these areas with greater precision (Fig.4a-b). Extracting information from these maps enables us to analyze the distribution and trends of structural changes with greater accuracy. The Tilt angle assists in understanding variations in the dip and deflection of layers, while the total horizontal derivatives of lineaments provide additional insights into magnetic field patterns and subsurface structures. This analytical approach can significantly aid in the more precise identification of boundaries and geological features within the region.

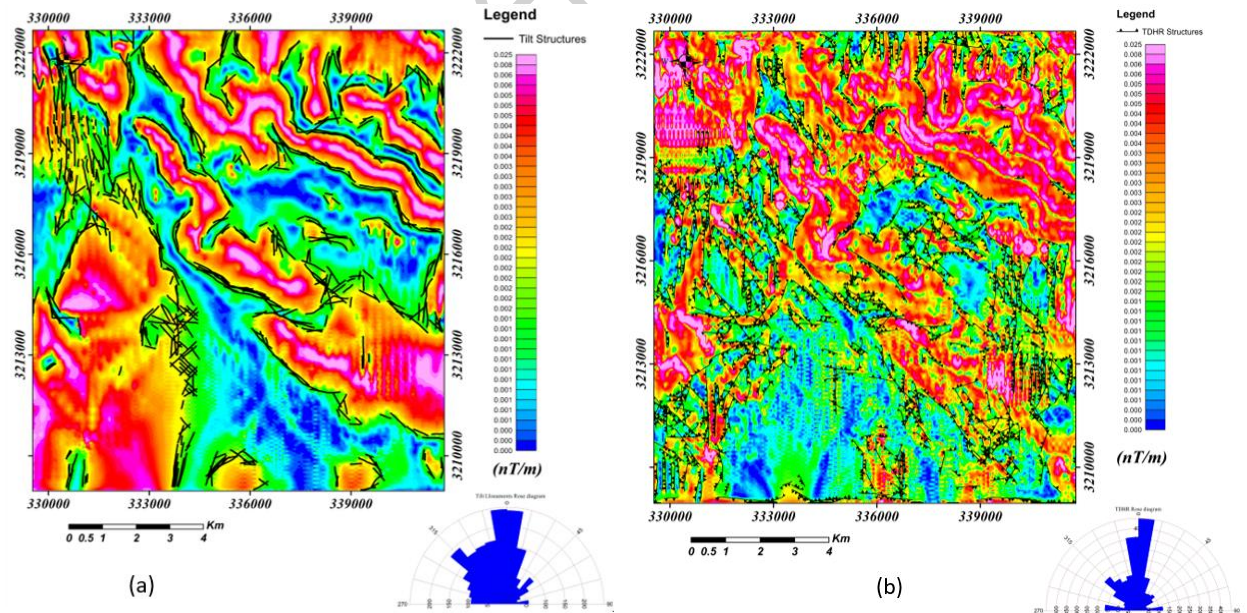


Figure 4. TDR and TDHR Filters Result; Fig.4a. TDR structures with Rose diagram; Fig.4b. TDHR structures with Rose diagram.

4.3. Euler Results

As illustrated in Figure 5, Euler deconvolution has been employed to extract magnetic contacts. This map depicts overarching trends in the primary structural indices, showcasing various depths and trends through the use of differently colored circles and diverse clustering. The Euler solutions presented in Figure 5 provide profound insights into the estimation of magnetic source depths. The Euler deconvolution method was applied to the airborne RTP magnetic data with a window size of 10x10 and a maximum depth tolerance of 10%. For SI=0, (figure. 5a), was designed to identify the locations of shallow contacts/faults, while SI=1 (figure. 5b), was employed to identify similar dike structures or deeper fault systems. Furthermore, the depth estimates derived from the colored circles align remarkably well with the components of the residual magnetic map (RES), (Fig. 2b).

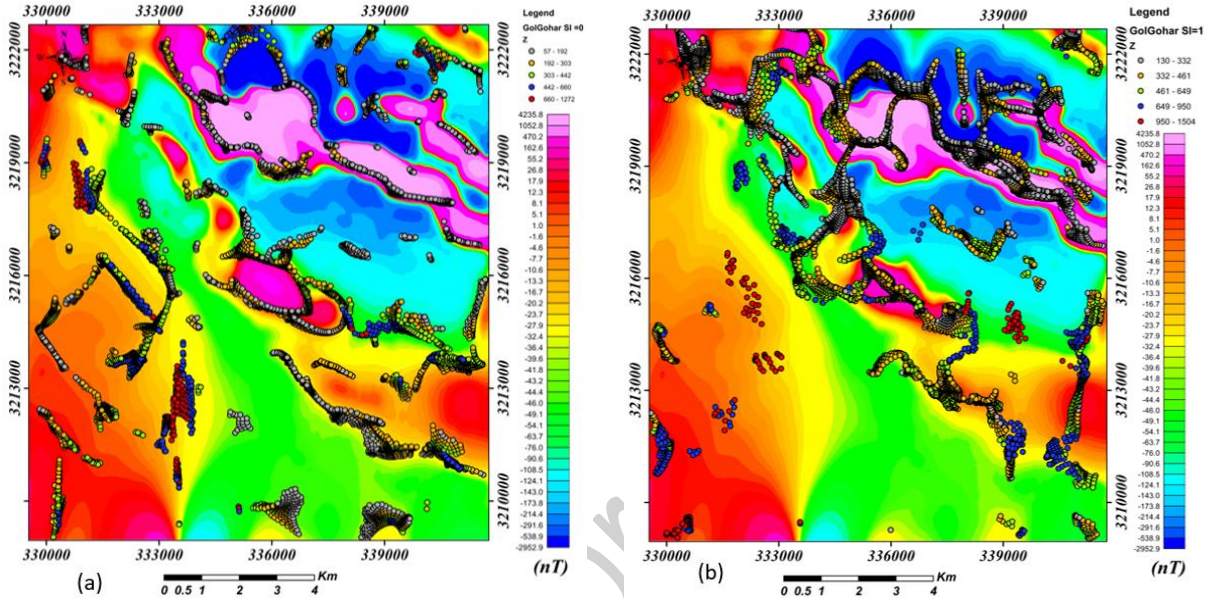


Figure.5. Gol Gohar Euler Depth Estimation dots; Fig.5a. Euler Depth Map, SI=0; Fig.5a. Euler Depth Map, SI=1

The surface and subsurface structures extracted through the Euler deconvolution method are illustrated in (Figures 5a and 5b). This analysis enables us to identify the depth and type of structures present in the study area. By establishing a Structural Index (SI=0), which indicates contacts, we can infer shallow depths of these structures. Conversely, employing an SI=1, indicative of (dyke/ sill) formations, reveals deeper structural features. The trend analysis of these structures indicates orientations of NW-SE, N-S, NE-SW, and E-W. The prevailing trend of the faults, as illustrated in Figures 5 is oriented along a NW-SE direction. Notably, these orientations align with the fault directions depicted on the geological map at a scale of 1: 25,000. This correlation may suggest tectonic activities and geological processes in the region that have significantly influenced the formation and development of subsurface structures. Consequently, the findings from this analysis not only elucidate the depth and nature of the structures but also enhance our understanding of the geological dynamics of the area, paving the way for further research and investigation in this domain. Figure 5 serves as a key reference in the analysis of geological structures, effectively illustrating depth and structural trends. The diagrams (Fig.6 a-b), derived from a profile with the trend of NW-SE on the Euler depth estimation grid, provide detailed insights into surface and subsurface structures and variations in depth through the application of deconvolution techniques. The horizontal axis represents geographical positions, while the vertical axis indicates changes in geological characteristics with depth.

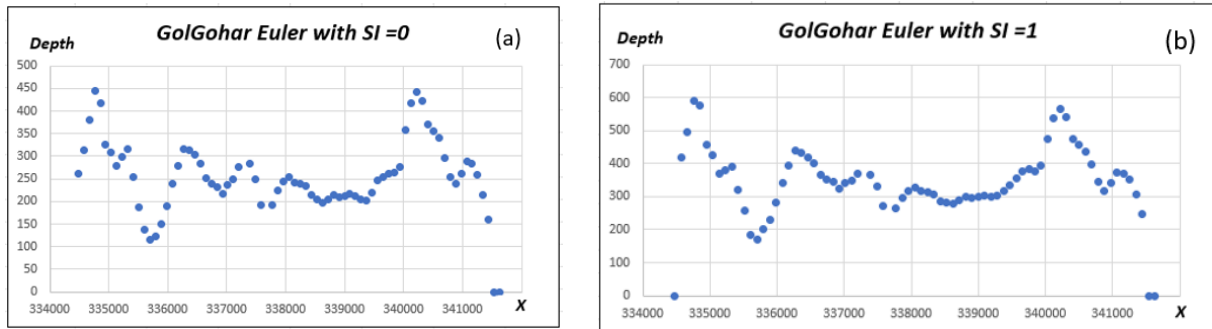


Figure.6. Gol Gohar Euler Depth Estimation Result on NW-SE profile, Figure.6. a Euler estimation with SI=0.5; Figure.6. b Euler estimation with SI=1.

Based on the analyses conducted from Figure 6A, it is observed that the depth of the structures begins at 100 meters and extends to a depth of 450 meters. The highest concentration of points is found within the depth range of 200 to 350 meters. Additionally, a clear trend of increasing depth from left to right is evident. In Figure 6B, the depth of the structures starts at 200 meters and continues to 700 meters, where again, the highest concentration of points is observed within the range of 300 to 500 meters. The trend of increasing depth in this diagram is also distinctly visible from left to right. Moreover, sudden changes in depth in several areas of these diagrams indicate the presence of faults and potential displacements related to magnetic anomalies. Although Profile A-B traverses only a specific point on the map and provides limited information, it has successfully yielded significant results. These results are consistent with the structures identified in the geological map at a scale of 1:25000 for the region. This consistency demonstrates the accuracy and reliability of the methods employed in geological analyses and can contribute to a deeper understanding of the structural features of the area.

5. Conclusion

This study investigates the surface and subsurface structures of the Gol Gohar mining area using airborne magnetic data as the primary research tool. Several advanced methods, including total horizontal derivatives (THDR), tilt angle derivatives (TDR), the analytical signal (AS) of magnetic data, and Euler deconvolution, were applied to analyze the region's structural framework.

The findings reveal that the geological structure of the area predominantly follows a northwest-southeast trend, which is disrupted by north-south-oriented faults. Depth analysis of these lineaments indicates the presence of ferromagnetic bodies at significant depths, extending from the northwest to the southeast. These results provide valuable insights into the structural complexity and depth of the region.

Notably, the consistency observed between derivative-based methods and Euler deconvolution techniques is striking. Both approaches identify surface and subsurface structures that align well with the boundaries of ferromagnetic anomalies, underscoring the reliability and robustness of the employed methods. This agreement not only affirms the credibility of the analyses but also highlights the potential for using these techniques in similar geological studies. To further enhance this research, it is recommended to incorporate 3D geophysical modeling techniques for a more detailed analysis of the location and geometry of the ferromagnetic bodies. Additionally, integrating magnetic data with seismic or gravity data could provide a more comprehensive understanding of the subsurface structures. This multi-method approach can reduce ambiguity in data interpretation and improve accuracy in identifying the depth and boundaries of the subsurface features.

References

1. Blakely, R.J., *Potential theory in gravity and magnetic applications*. 1996: Cambridge university press.
2. Verduzco, B., et al., *New insights into magnetic derivatives for structural mapping*. 2004. **23**(2): p. 116-119.

3. Fairhead, J. and S. Williams, *Evaluating normalized magnetic derivatives for structural mapping*, in *SEG Technical Program Expanded Abstracts 2006*. 2006, Society of Exploration Geophysicists. p. 845-849.
4. Sultan, S., et al., *Geophysical measurements for subsurface mapping and groundwater exploration at the central part of the Sinai Peninsula, Egypt*. 2009. **34**(1): p. 103.
5. Holden, E.-J., et al. *Detection of regions of structural complexity within aeromagnetic data using image analysis*. in *2010 25th International Conference of Image and Vision Computing New Zealand*. 2010. IEEE.
6. Oruç, B. and H.J.J.o.A.G. Selim, *Interpretation of magnetic data in the Sinop area of Mid Black Sea, Turkey, using tilt derivative, Euler deconvolution, and discrete wavelet transform*. 2011. **74**(4): p. 194-204.
7. Ferreira, F.J., et al., *Enhancement of the total horizontal gradient of magnetic anomalies using the tilt angle*. 2013. **78**(3): p. J33-J41.
8. Beamish, D. and J. White, *TellusSW: airborne geophysical data and processing report*. 2014.
9. Dentith, M. and S.T. Mudge, *Geophysics for the mineral exploration geoscientist*. 2014: Cambridge University Press.
10. Khalil, M.H.J.J.o.A.G., *Subsurface faults detection based on magnetic anomalies investigation: a field example at Taba protectorate, South Sinai*. 2016. **131**: p. 123-132.
11. Nasuti, Y. and A.J.G.J.I. Nasuti, *NTilt as an improved enhanced tilt derivative filter for edge detection of potential field anomalies*. 2018. **214**(1): p. 36-45.
12. Ibraheem, I.M., M. Haggag, and B.J.G. Tezkan, *Edge detectors as structural imaging tools using aeromagnetic data: A case study of Sohag Area, Egypt*. 2019. **9**(5): p. 211.
13. Cheng, Q. and Y. Xu. *Geophysical data processing and interpreting and for mineral potential mapping in GIS environment*. in *Proceedings of the Fourth Annual Conference of the International Association for Mathematical Geology*. 1998. De Frede Editore Napoli, Italy.
14. Siemon, B. and T. Kerner. *Airborne Geophysical Investigation of the Environment of Abandoned Salt Mines along the Staßfurt-Egeln Anticline, German*. in *73rd EAGE Conference and Exhibition incorporating SPE EUROPEC 2011*. 2011. European Association of Geoscientists & Engineers.
15. Siemon, B., M. Ibs-von Seht, and S.J.R.S. Frank, *Airborne electromagnetic and radiometric peat thickness mapping of a bog in Northwest Germany (Ahlen-Falkenberger Moor)*. 2020. **12**(2): p. 203.
16. Toktay, H.D.J.A.i.M.S. and Applications, *INTERPRETATION OF MAGNETIC ANOMALIES BY USING ASTA EDGE DETECTION METHOD: SAKARYA (SAPANCA) EXAMPLE*. 2021. **30**(2).
17. Zhao, Y., et al., *A brief review of magnetic anomaly detection*. 2021. **32**(4): p. 042002.
18. Ghorbani, M., *The geology of Iran: tectonic, magmatism and metamorphism*. 2021: Springer.
19. Mirzaei, R., et al., *Two-tiered magmatic-hydrothermal and skarn origin of magnetite from Gol-Gohar iron ore deposit of SE Iran: in-situ LA-ICP-MS analyses*. 2018. **102**: p. 639-653.
20. Ghalamghash, J.K., A, *Gol Gohar geological map 1:25000*. Geological Survey of Iran, 2014.
21. Sabzehi, M.J.G.s.o.I., Tehran, *Gol Gohar geological map 1: 100000*. 1997.
22. Dentith, M., D.R. Cowan, and L.A.J.E.G. Tompkins, *Enhancement of subtle features in aeromagnetic data*. 2000. **31**(2): p. 104-108.
23. Jacobsen, B.H.J.G., *A case for upward continuation as a standard separation filter for potential-field maps*. 1987. **52**(8): p. 1138-1148.
24. Salem, A., et al., *Interpretation of magnetic data using tilt-angle derivatives*. 2008. **73**(1): p. L1-L10.
25. Keating, P. and L.J.G. Zerbo, *An improved technique for reduction to the pole at low latitudes*. 1996. **61**(1): p. 131-137.
26. Li, X.J.T.I.e., *Magnetic reduction-to-the-pole at low latitudes: Observations and considerations*. 2008. **27**(8): p. 990-1002.

27. Phillips, J.D., *Locating magnetic contacts: a comparison of the horizontal gradient, analytic signal, and local wavenumber methods*, in *SEG Technical Program Expanded Abstracts 2000*. 2000, Society of Exploration Geophysicists. p. 402-405.
28. Reilly, A., G. Frazer, and B.J.I.T.o.S.P. Boashash, *Analytic signal generation-tips and traps*. 1994. **42**(11): p. 3241-3245.
29. Miller, H.G. and V.J.J.o.a.G. Singh, *Potential field tilt—a new concept for location of potential field sources*. 1994. **32**(2-3): p. 213-217.
30. Hood, P.J.G., *Gradient measurements in aeromagnetic surveying*. 1965. **30**(5): p. 891-902.
31. Thompson, D.J.G., *EULDPH: A new technique for making computer-assisted depth estimates from magnetic data*. 1982. **47**(1): p. 31-37.
32. Keating, P. and M.J.G.p. Pilkington, *Euler deconvolution of the analytic signal and its application to magnetic interpretation*. 2004. **52**(3): p. 165-182.
33. Bultman, M.W., *Detailed interpretation of aeromagnetic data from the Patagonia Mountains area, southeastern Arizona*. 2015, US Geological Survey.
34. Reid, A.B., et al., *Magnetic interpretation in three dimensions using Euler deconvolution*. 1990. **55**(1): p. 80-91.
35. Elhussein, M., et al., *Aeromagnetic Data Analysis for Sustainable Structural Mapping of the Missiakat Al Jukh Area in the Central Eastern Desert: Enhancing Resource Exploration with Minimal Environmental Impact*. 2024. **16**(20): p. 8764.